A&A 437, 553–560 (2005)
DOI: 10.1051/0004-6361:20042328

Astronomy & Astrophysics

Asteroseismic tests of element diffusion in solar type stars

S. Théado[1,2], S. Vauclair[3], M. Castro[3], S. Charpinet[3], and N. Dolez[3]

[1] Université de Liège, allée du 6 Août 17, 4000 Liège, Belgium
[2] Centro de Astrofisica da Universidade do Porto, Rua das Estrelas, 4150-762 Porto, Portugal
[3] Laboratoire d'Astrophysique, 14 Av. Ed. Belin, 31400 Toulouse, France
e-mail: svcr@ast.obs-mip.fr

Received 8 November 2004 / Accepted 21 February 2005

Abstract. Following the success of helioseismology, asteroseismology is now becoming a fundamental tool for penetrating the secrets of the internal structure of stars. In preparation of this new era in stellar physics, we study the effects of element diffusion on the computed frequencies of stellar oscillation modes for main-sequence solar-type stars. As the observed stars will be constrained by their atmospheric parameters, stellar models were computed with different physical inputs (whether including element diffusion or not) and iterated in order to fit the same observables (effective temperature, luminosity, surface chemical composition). The theoretical oscillation frequencies of these models were derived and compared. The results show that diffusion alters the internal structure of the models and their oscillation frequencies in a significant way. Although observational uncertainties in stellar external parameters are still important, comparisons between oscillation frequencies observed with the future space mission COROT and theoretically computed ones might provide evidence for diffusion processes in solar type stars.

Key words. diffusion – hydrodynamics – stars: abundances – stars: interiors – stars: oscillations (including pulsations)

1. Introduction

Asteroseismology will soon become an excellent tool for determining the internal structure of stars. New instruments and international collaborations are being settled for this purpose. Let us quote the HARPS spectrograph on the 3.60 m telescope in La Silla[1], the UCLES spectrograph on the Anglo Australian Telescope[2], the Canadian satellite MOST[3] and the space project COROT to be launched in 2006[4]. These missions will provide very precise determinations of oscillation frequencies, which will enable stellar physicists to test the physical inputs of their models. Among the important physical processes that occur in stars is the so-called "element diffusion", i.e. the relative separation of the various elements caused by gravitational and thermal settling, on the one hand, and radiative acceleration on the other. This process, which was described by Michaud (1970) to account for the abundance anomalies observed in chemically peculiar A stars, is now recognized as occuring in all kinds of stars. Its influence on the observed chemical abundances is extremely variable, however, due to competing macroscopic motions like convective mixing or rotation-induced turbulence (Turcotte et al. 1998; Richer et al. 2000; Théado & Vauclair 2003).

In the Sun, no observable abundance anomalies are expected from element diffusion, as the time scale of the process is longer than the solar lifetime. However the small induced depletion of helium and heavy elements by about 20% is detectable through helioseismology (Gough 1984; Libbrecht et al. 1990; Christensen-Dalsgaard & Pérez Hernández 1991; Dziembowski et al. 1991; Vorontsov et al. 1991; Kosovichev et al. 1992). Such detections are more difficult in stars, as only global oscillation modes can be detected, in contrast to the Sun, where local oscillations of the surface can be analyzed. Asteroseismic tests of the internal structure of stars have already been discussed by many authors (e.g. Gough 1990; Monteiro & Thompson 1998; Roxburgh & Vorontsov 2001; Mazumdar & Antia 2001; Miglio et al. 2003). Recently Vauclair & Théado (2004) have shown how helium gradients could be detectable in A-type stars, and Bazot & Vauclair (2004) have discussed asteroseismic tests of accretion. Here we turn to the question of element diffusion in solar type stars. Will its effect be detectable with instruments like COROT? What will the best asteroseismic tests be?

To tentatively answer this question, we computed pairs of stellar models with similar external parameters (luminosities, effective temperatures, and chemical composition), but in each case element diffusion is introduced in one of the models, but not in the other. Inside each pair, the stars would be undistinguishable by observation, except through asteroseismology.

In Sect. 2, we present our models and discuss differences in their internal structures; the consequences on the oscillation

[1] http://www.ls.eso.org/lasilla/sciops/3p6/harps
[2] http://www.ast.cam.ac.uk/AAO/astro/ucles.html
[3] http://wombat.astro.ubc.ca/MOST/
[4] http://smsc.cnes.fr/COROT/

Table 1. Characteristics of the models; α: mixing length parameter; Y_0: original helium mass fraction; X_S and Y_S: surface hydrogen and helium mass fractions.

Models	α	Y_0	$L/L_\odot$	$\lvert\Delta L\rvert/L$	$T_{\rm eff}$ (K)	$\lvert\Delta T\rvert/T$	X_s	Y_s
M1-hom	1.753739	0.268039	1.45332		6103.08		0.7145	0.2680
M1-dif	1.838081	0.267100	1.45348	0.011%	6102.89	0.0031%	0.7431	0.2404
M2-hom	1.753739	0.268039	2.36668		6363.86		0.7145	0.2680
M2-dif	1.884184	0.267591	2.36755	0.042%	6361.08	0.044%	0.7708	0.2137
M3-hom	1.753739	0.268039	3.54022		6478.44		0.7145	0.2680
M3-dif	1.995200	0.268238	3.54030	0.0023%	6478.87	0.0066%	0.8164	0.1696

Table 2. Characteristics of the models (continued); t_*: acoustic radius; r_{cz}: radius at the bottom of the surface convective zone; τ_{cz}: acoustic depth of the convective zone; r_{cc}: radius at the top of the convective core; t_{cc}: acoustic radius of the convective core.

Models	R_* (10^{10} cm)	t_* (s)	r_{cz}/R_*	τ_{cz} (s)	r_{cc}/R_*	t_{cc} (s)
M1-hom	7.54	3784.6	0.775	2004.5	–	–
M1-dif	7.54	3784.2	0.767	2037.6	–	–
M2-hom	8.66	4466.6	0.810	2172.7	0.041	64.7
M2-dif	8.66	4466.5	0.797	2247.8	0.044	70.9
M3-hom	10.0	5390.3	0.849	2323.4	0.066	120.9
M3-dif	10.0	5377.4	0.831	2458.7	0.067	124.0

frequencies and the asteroseismic tests are presented in Sect. 3; in Sect. 4 the importance of uncertainties on the observed parameters is discussed, and finally Sect. 5 is devoted to the discussion and concluding remarks.

2. Differences in the internal structure of the models

2.1. Computations, calibration, and characteristics of the models

We computed stellar models with the Toulouse-Geneva evolutionary code for several masses: 1.1, 1.2, and 1.3 $M_\odot$, respectively noted M1, M2, and M3. For a given stellar mass, we computed two series of models: with and without element diffusion. The series were calibrated to obtain pairs of models with the same effective temperatures, luminosities, and chemical composition, except helium which is not directly observable in these solar-type stars. This calibration was achieved by adjusting the two free parameters of the stellar evolution code: the initial helium abundance Y_0 and the mixing length parameter α. For each pair, the two models lie at the same point on the HR diagram.

Changing one of these two parameters affects both the luminosity and effective temperature of the model at a given age, while both decrease with the mixing length parameter. At the same time, increasing the initial helium abundance leads to a decrease in the luminosity and the effective temperature. The effective temperature is particularly sensitive to the mixing length parameter, while the luminosity strongly depends on the initial helium abundance. Consequently for given values of L and $T_{\rm eff}$, the mixing length parameter and the initial helium abundance, which together lead to well-calibrated models, are unique. The relation between (L, $T_{\rm eff}$) and (α, Y_0) is not linear and depends on the stellar parameters (mass, age): hence, no simple analytical relation between these parameters can be found. For masses above 1.3 $M_\odot$, both L and $T_{\rm eff}$ strongly depend on the two parameters, so that the calibration is still more difficult to obtain.

Tables 1 and 2 give the characteristics of our models with and without diffusion for each mass. For the three "homogeneous models" (i.e. without diffusion), we used the same values of the free parameters α and Y_0. Models including diffusion are then calibrated to find the same values of the external parameters as the homogeneous ones. The tables show that the calibrated models do not have strictly identical values of the surface parameters but are indeed very close.

Figure 1 displays the evolutionary tracks. For each mass the tracks for models with and without diffusion are very close along most of the evolution on the main-sequence.

2.2. Computational results

Figures 2 to 4 compare the internal structures of models with and without diffusion: density, pressure, temperature, square sound velocity. They show that microscopic diffusion leads to variations of the stellar structure, which are uniform in the convective regions, while in radiative zones the effect depends on depth. Diffusion hardly alters the sound speed profile in the convective zone (except just below the surface), while its

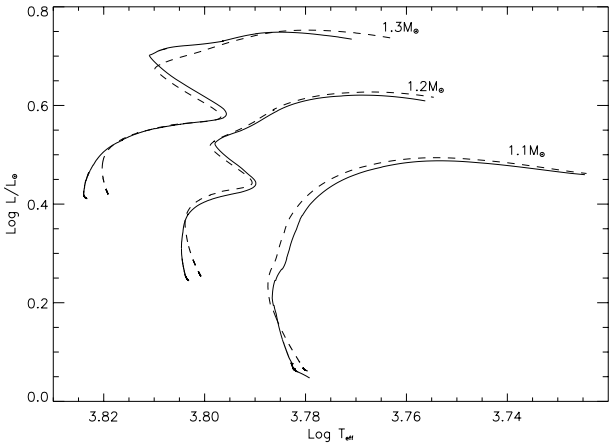

Fig. 1. Evolutionary tracks of the 1.1, 1.2, and 1.3 $M_\odot$ models. Dashed line: standard homogeneous models (without microscopic diffusion), solid line: models including microscopic diffusion.

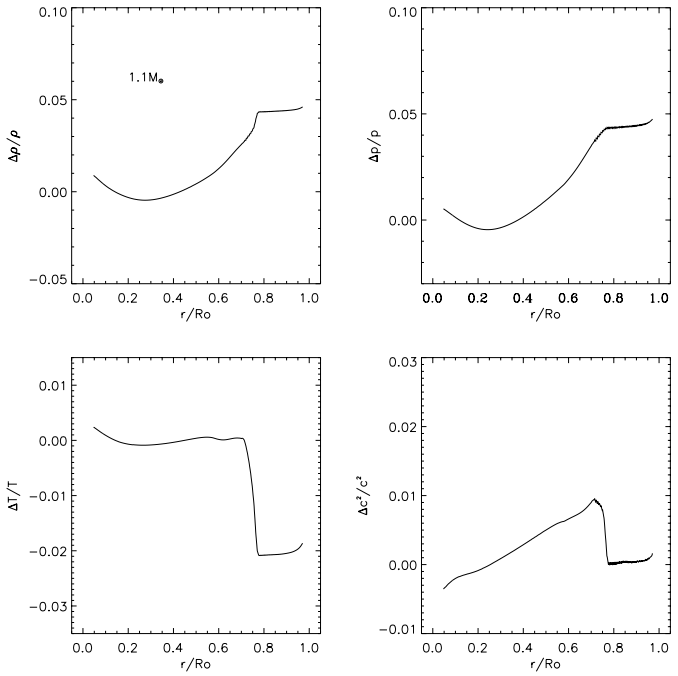

Fig. 2. Comparison between 1.1 $M_\odot$ models with and without microscopic diffusion: density, pressure, temperature, and relative differences in sound speed between M1-hom and M1-dif (e.g: $\Delta c^2/c^2 = (c^2_{\rm dif} - c^2_{\rm hom})/c^2_{\rm hom}$).

effects are large on the structure of the radiative interior. In the radiative region $\Delta c^2/c^2$ strongly varies with depth.

3. Asteroseismic tests

3.1. Oscillation frequencies

We computed the theoretical oscillation frequencies of our models, using an updated version of the adiabatic code described in Brassard et al. (1992), for different values of the angular degree l and the radial order n. Figures 5 to 7 compare the oscillation frequencies of the two models for each mass. We observe different $\Delta\nu/\nu$ behaviors at low and high n values.

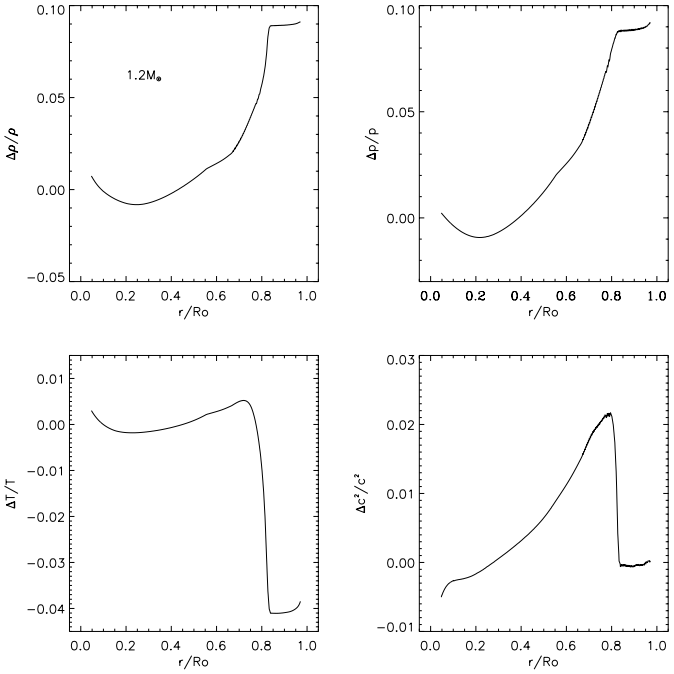

Fig. 3. Comparison between 1.2 $M_\odot$ models with and without microscopic diffusion: density, pressure, temperature, and relative differences in sound speed between M2-hom and M2-dif (e.g.: $\Delta c^2/c^2 = (c^2_{\rm dif} - c^2_{\rm hom})/c^2_{\rm hom}$).

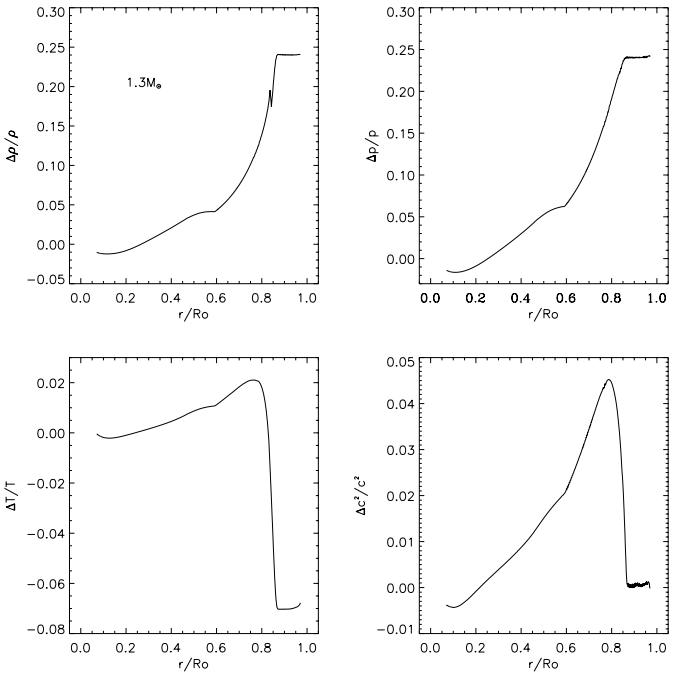

Fig. 4. Comparison between 1.3 $M_\odot$ models with and without microscopic diffusion: density, pressure, temperature and relative differences in sound speed between M3-hom and M3-dif (e.g.: $\Delta c^2/c^2 = (c^2_{\rm dif} - c^2_{\rm hom})/c^2_{\rm hom}$).

For large n values, relative differences between the frequencies of the two models are nearly constant. For small n values, the $\Delta\nu/\nu$ variations are much larger.

Figure 8 displays the eigenfunctions ξ_r (radial motion) in 1.2 $M_\odot$ models for two modes with the same degree ($l = 2$)

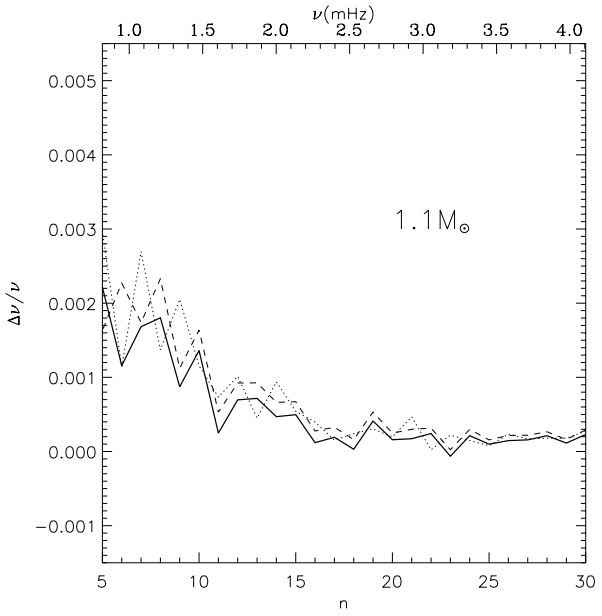

Fig. 5. Comparison between oscillation frequencies of 1.1 $M_\odot$ models with (M1-dif) and without microscopic diffusion (M1-hom): $\Delta\nu/\nu = (\nu_{\rm diff} - \nu_{\rm hom})/\nu_{\rm hom}$. Solid curve: $l = 0$, dashed curve: $l = 1$, dotted curve: $l = 2$.

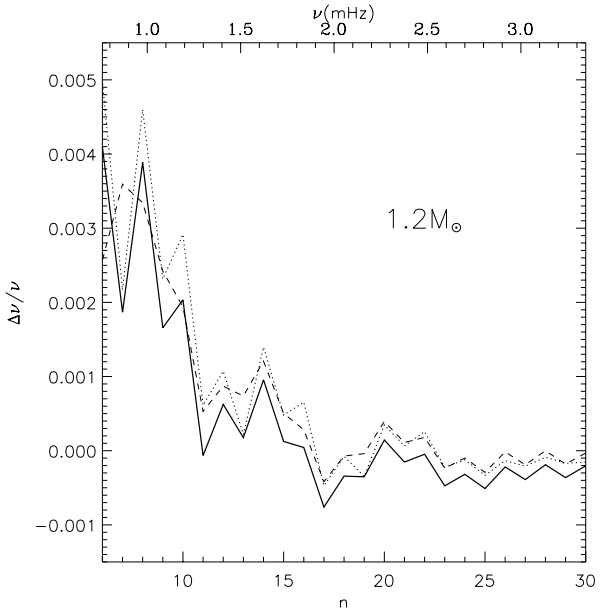

Fig. 6. Comparison between oscillation frequencies of 1.2 $M_\odot$ models with (M2-dif) and without microscopic diffusion (M2-hom): $\Delta\nu/\nu = (\nu_{\rm diff} - \nu_{\rm hom})/\nu_{\rm hom}$. Solid curve: $l = 0$, dashed curve: $l = 1$, dotted curve: $l = 2$.

but with a different radial order, $n = 9$ and $n = 20$. In both cases the amplitude of the wave decreases with depth, but for $n = 20$ the decrease is much faster than for $n = 9$. Modes with a low n number propagate deeper with a non-negligible amplitude than those with larger n values; in other words, the relative sensitivity of the modes to the structure of deepest lying layers increase with frequency. According to Figs. 5–7, the relative differences between the frequencies of the waves with large n (or frequency) values are nearly constant, due to

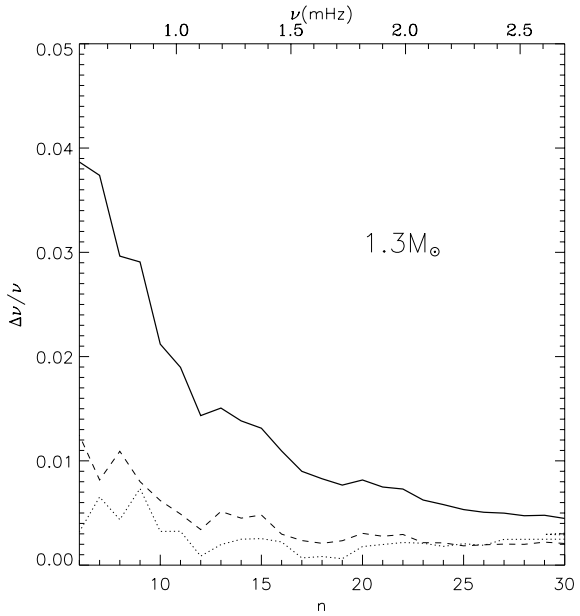

Fig. 7. Comparison between oscillation frequencies of 1.3 $M_\odot$ models with (M3-dif) and without microscopic diffusion (M3-hom) (at =2.320 Gyrs): $\Delta\nu/\nu = (\nu_{\rm diff} - \nu_{\rm hom})/\nu_{\rm hom}$. Solid curve: $l = 0$, dashed curve: $l = 1$, dotted curve: $l = 2$.

the small uniform difference $\Delta c^2/c^2$ observed in the convective zone. On the other hand, the $\Delta\nu/\nu$ behaviors are different for small n values: the corresponding waves propagate with a non negligible amplitude through the radiative interior as well. The corresponding $\Delta\nu/\nu$ differences are due to the larger $\Delta c^2/c^2$ observed in the radiative interior.

While comparing observed and computed oscillation frequencies, a difficulty occurs due to an unknown phase term induced by the reflexion of the waves at the surface. For this reason, frequency differences are better tests than absolute values (e.g. Gough 1990; Christensen-Dalsgaard 2002). As discussed in detail by Roxburgh & Vorontsov (2001, 2003), the so-called "small spacings" are good tests of stellar cores. On the other hand, the features that occur in stellar outer layers are better probed by the so-called "second differences" (Gough 1990; Monteiro & Thompson 1998; Vauclair & Théado 2004), as discussed below.

3.2. Frequency separations and differences

Here we discuss the various asteroseismic tests of diffusion. The most important differences between the models with and without diffusion lie in and just below the convective zone. For this reason we investigate the behavior of the sound velocity due to helium depletion and its consequences.

Figure 9 displays the helium profiles in the models with and without diffusion as a function of the acoustic depth, time needed for the waves to travel from the surface down to the considered layer. The helium gradients due to diffusion are clearly seen. Figure 10 displays the gradient of the sound velocity as a function of the acoustic depth. The features around 500 s are caused by the helium ionisation zones which lead to well-known bumps in the thermodynamical coefficient Γ_1 (Fig. 11).

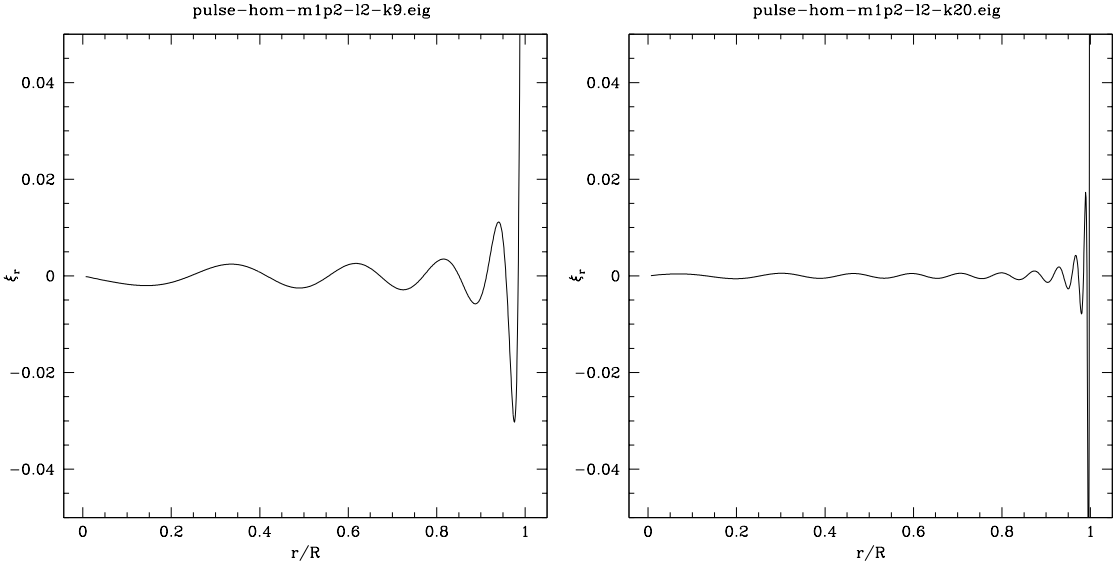

Fig. 8. Radial displacement eigenfunction for two (l = 2) modes in a 1.2 $M_\odot$ model. On the left: n = 9 , on the right: n = 20.

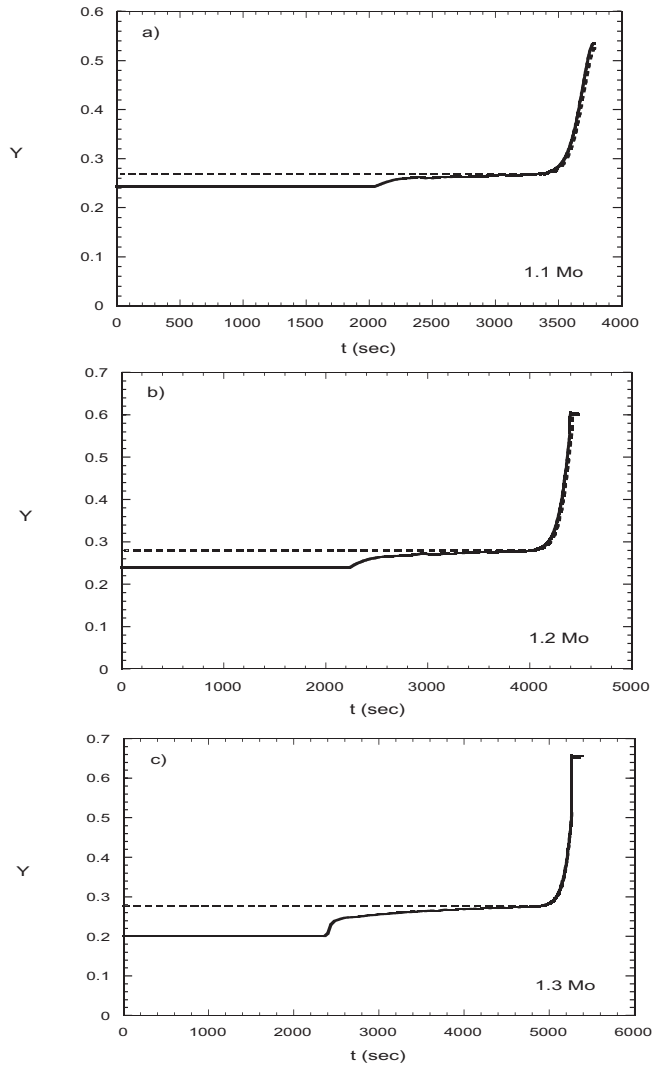

Fig. 9. Helium profiles in **a)** 1.1 $M_\odot$, **b)** 1.2 $M_\odot$, **c)** 1.3 $M_\odot$ models with diffusion (solid lines) or without diffusion (dashed lines). In abscissae the acoustic depths in the models are plotted, i.e. the time needed for the acoustic waves to travel from the surface down to the considered layer.

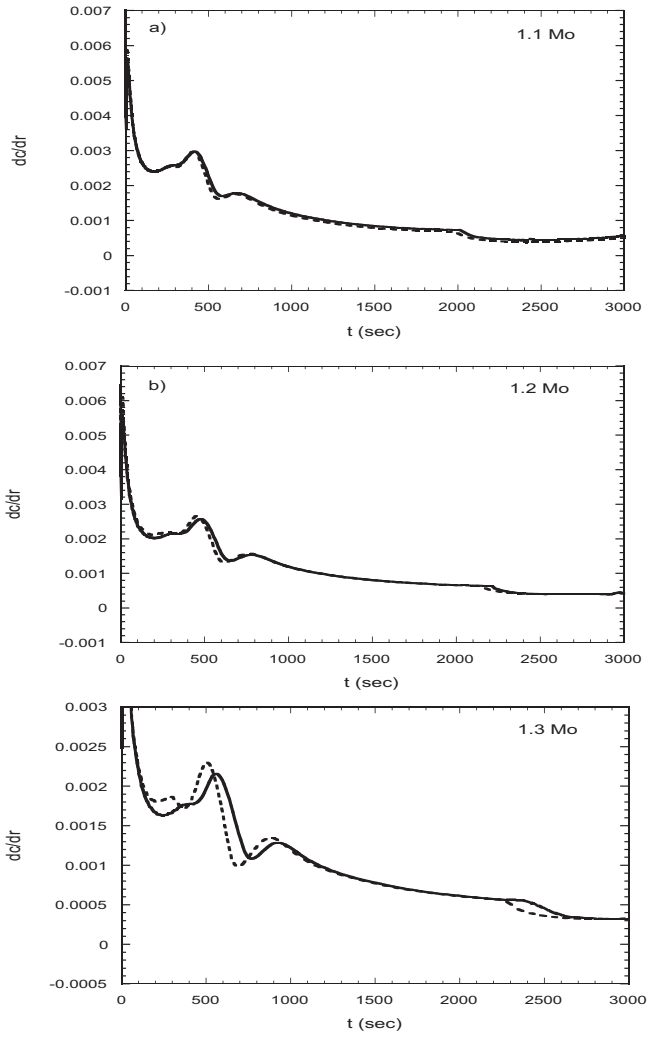

Fig. 10. Gradient of the sound velocity in the same models (**a**), **b**), **c**)) as Fig. 9.

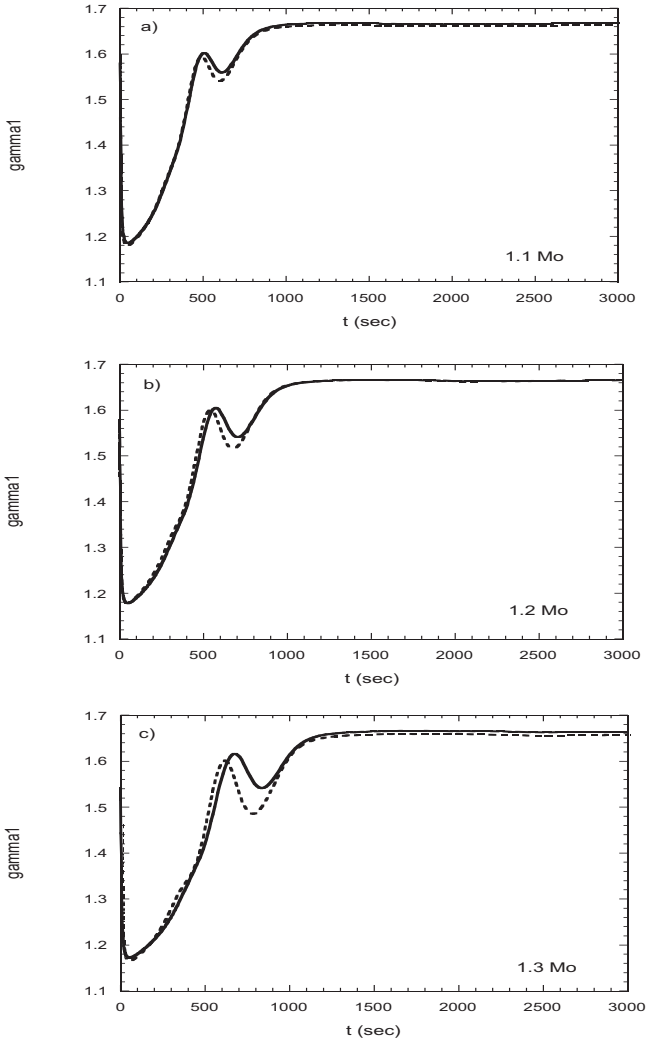

Fig. 11. Γ_1 profiles in the same models (**a**), **b**), **c**)) as Fig. 9.

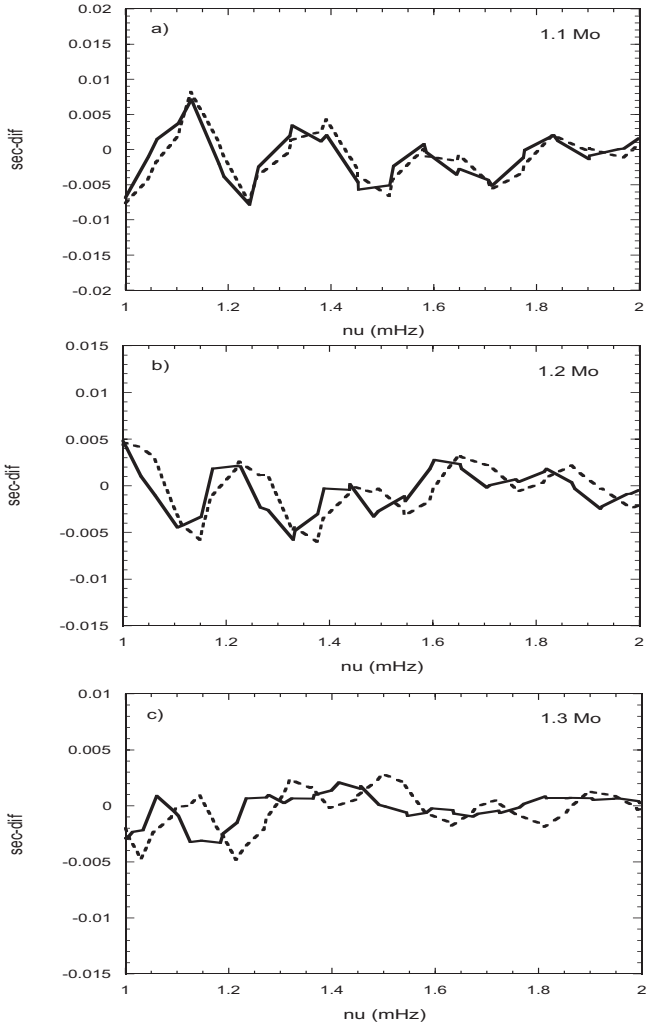

Fig. 12. Second differences in the same models (**a**), **b**), **c**)) as Fig. 9.

The bottom of the convective zones also leads to characteristic features at $t \simeq 2000$ s (1.1 $M_\odot$), 2200 s (1.2 $M_\odot$), and 2300 s (1.3 $M_\odot$). The differences between the models with and without diffusion increase with the stellar mass and are clearly visible in the 1.3 $M_\odot$ models (Fig. 10c).

Due to the partial reflection of the pressure waves on the regions of rapid variations in the sound velocity, the computed frequencies present characteristic oscillations that are better seen in the "second differences" (Gough 1990; Monteiro & Thompson 1998; Vauclair & Théado 2004):

$$\delta_2 \nu = \nu_{n+1} + \nu_{n-1} - 2\nu_n. \quad (1)$$

The second differences for our models are presented in Fig. 12. The Fourier transforms of these curves are shown in Fig. 13. As discussed in details by Vauclair & Théado (2004), the position of the peaks correspond to twice the acoustic depth of the corresponding feature in the sound velocity. By comparison with Fig. 10, one can easily recognize the peaks due to the helium ionisation zones and those due to the bottom of the convective zones. In the 1.3 $M_\odot$ models, the difference between the two cases is clearly visible: for models with diffusion, the feature due to the helium ionisation zones is smaller and the convective depth larger than for the case without diffusion. This last result seems a priori to contradict the fact that helium depletion in a stellar model leads to regression of the helium induced convection zone (Vauclair et al. 1974). However the situation is different here as the models are consistently iterated to appear at the same place in the HR diagram: in this case the convective zone is deeper in the model with diffusion.

We also studied the effect of diffusion on the small frequency spacings, which are more sensitive to the deep stellar interior (Tassoul 1980; Roxburgh & Vorontsov 2001, 2003):

$$\delta\nu = \delta\nu_{n,l} - \nu_{n-1,l+2}. \quad (2)$$

These quantities may be good tests of the deep internal differences between models with and without diffusion. We computed the small spacings for $l = 0$ and 2, on the one hand, $l = 1$ and 3, on the other. We found a significant effect for the 1.3 $M_\odot$ models, as presented in Fig. 14. We can see that for the $l = 0$, 2 case the small spacings are larger in the model with diffusion than in the model without diffusion, while it is the contrary for the $l = 1$, 3 case. The differences are approximately 1–2 μHz.

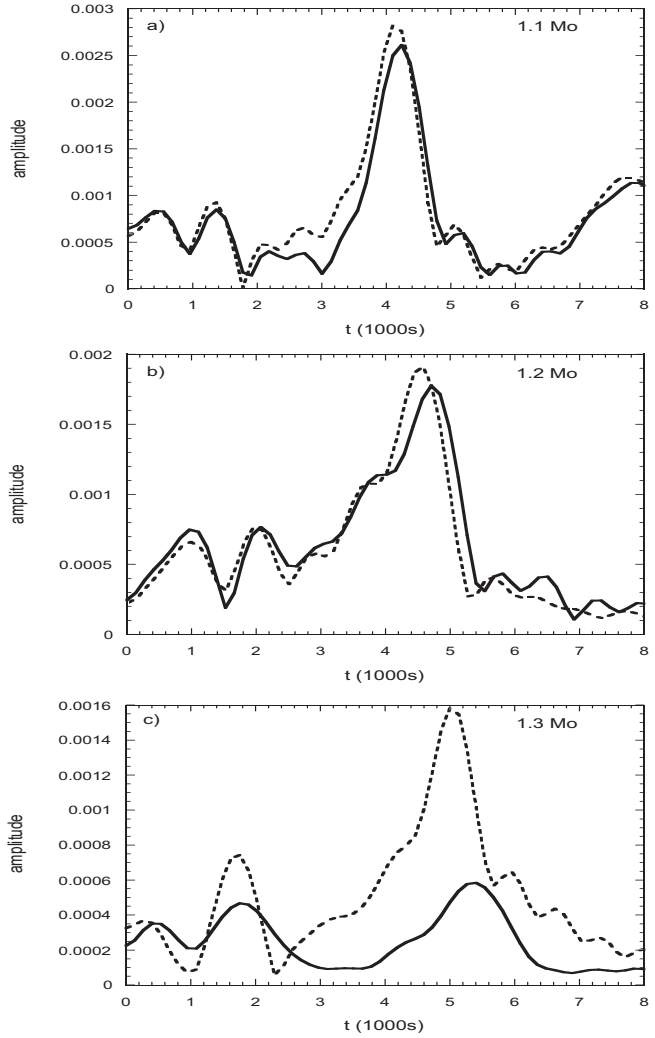

Fig. 13. Fourier transform of the second differences in the same models (**a**), **b**), **c**)) as Fig. 9.

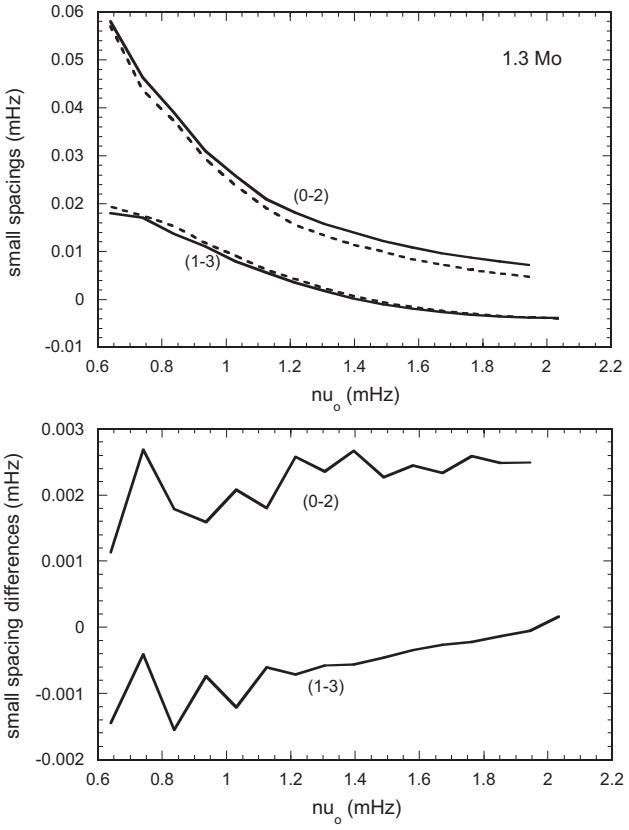

Fig. 14. *Top*: small frequency spacings in the 1.3 $M_\odot$ models with diffusion (solid lines) or without diffusion (dashed lines). The curves are labelled according to the l values (0, 2) or (1, 3). *Bottom*: differences between the small spacings for models with diffusion minus those for models without diffusion, as presented in the top graph.

4. Discussion

The diffusion-induced effects on stellar oscillation frequencies have been tested in solar-type stars of masses 1.1 to 1.3 $M_\odot$. We compared stellar models with very close values of M, L, $T_{\rm eff}$, $X_{\rm surf}$, and $Y_{\rm surf}$ (i.e. at same point in the HR diagram), computed with or without element diffusion. Considering the classical stellar observables, the models with and without diffusion can account for the same observed star but the presence or absence of diffusion makes their internal structures different. The resulting frequency differences were studied, and show different behaviors for modes with low and high values of the radial order n. For modes with high n values, the differences in the frequency values hardly vary with radial order. For modes with small values of n (i.e. modes which propagate through the radiative zone with a non negligeable amplitude) the $\Delta\nu/\nu$ variations with n are much larger.

We studied the effect of element diffusion on the second differences, which are good tests of the helium ionisation regions and of the depth of the convective zones. We also studied the small frequency spacings, which are more sensitive to the deep internal structure. Differences between the models with and without diffusion increase with stellar mass and should be detectable with instruments like COROT, at least for stars of 1.3 $M_\odot$. The frequency differences ($\Delta\nu$) between models with and without diffusion are on the order of several microHertz, while the accuracy of COROT is expected to reach 0.1 μHz (C. Catala, private communication). Element diffusion clearly has to be taken into account in comparisons between models and observations of solar-type stars, as their influence on frequencies is larger than the expected instrumental accuracy. For hotter stars, the radiative acceleration on metals, which was not introduced in the present computations, can lead to metal accumulation in specific stellar layers. Asteroseismology will become an important tool for trying to localize these chemical inhomogeneities, which will be studied in future work.

Acknowledgements. This work was partially supported by a grant POCTI/1999/FIS/34549 approved by FCT and POCTI, with funds from the European Community programme FEDER Sylvie Vauclair acknowledges a grant from Institut universitaire de France.

References

Bazot, M., & Vauclair, S. 2004, A&A, 427, 965

Brassard, P., Pelletier, C., Fontaine, G., & Wesemael, F. 1992, ApJS, 80, 725

Christensen-Dalsgaard, J., & Pérez Hernández, F. 1991, in Challenges to theories of the structure of moderate-mass stars, ed. D. O. Gough, & J. Toomre (Heildelberg: Springer), 43

Christensen-Dalsgaard, J. 2002, RvMP, 74, 1073C

Dziembowsky, W. A., Pamyatnykh, A. A., & Sienkiewicz, R. 1991, MNRAS, 249, 602

Gough, D. O. 1984, Mem. Soc. Astron. It., 55, 13

Gough, D. O. 1990, in Progress of Seismology of the Sun and Stars, Proc. Oji International Seminar, Hakone (Japan: Springer Verlag), ed. Y. Osaki, & H. Shibahashi, Lect. Notes Phys., 367, 283

Kosovichev, A. G., Christensen-Dalsgaard, J., & Dziembowski, W. A. 1992, MNRAS, 259, 536

Libbrecht, K. G., Woodard, M. F., & Kaufman, J. M. 1990, ApJS, 74, 1129

Mazumdar, A., & Antia, H. M. 2001, A&A, 377, 192

Michaud, G. 1970, ApJ, 160, 641

Miglio, A., Christensen-Dalsgaard, J., Di Mauro, M. P., Monteiro, M. J. P. F. G., & Thompson, M. J. 2003, in Asteroseismology across the HR diagram, ed. M. J. Thompson, M. S. Cunha, & M. J. P. F. G. Monteiro (Dordrecht: Kluwer), 537

Monteiro, M. J. P. F. G., & Thompson, M. J. 1998, in New eyes to see inside the Sun and Stars (Dordrecht: Kluwer), ed. F.-L. Deubner, J. Christensen-Dalsgaard, & D. W. Kurtz, Proc. IAU Symp., 185, 317

Richer, J., Michaud, G., & Turcotte, S. 2000, ApJ, 529, 338

Roxburgh, I. W., & Vorontsov, S. V. 2001, MNRAS, 322, 85

Roxburgh, I. W., & Vorontsov, S. V. 2003, A&A, 411, 215

Tassoul, M. 1980, ApJS, 43, 469

Théado, S., & Vauclair, S. 2003, ApJ, 587, 795

Turcotte, S., Richer, J., & Michaud 1998, ApJ, 504, 559

Vauclair, S., & Théado, S. 2004, A&A, 425, 179

Vauclair, G., Vauclair, S., & Pamjatnikh, A. 1974, A&A, 31, 63

Vorontsov, S. V., Baturin, V. A., & Pamyatnykh, A. A. 1991, Nature, 349, 49